EUROPEAN ORGANIZATION FOR NUCLEAR RESEARCH

L3 Note 2565
June 29, 2000

Beauty Production in $\gamma\gamma$ Collisions at LEP

L3 Collaboration

Abstract

The production of b quarks in $\gamma\gamma$ collisions is studied with the L3 detector at LEP. The data sample used corresponds to a total integrated luminosity of 410 pb^{-1}, collected at centre-of-mass energies from 189 GeV to 202 GeV. Hadronic final states containing b quarks are identified by detecting electrons or muons from their semi-leptonic decay. The cross section $\sigma(e^+e^- \rightarrow e^+e^- b\bar{b}X)$ is compared to perturbative next-to-leading order QCD calculations. The cross section of b production is measured in $\gamma\gamma$ collisions for the first time.

Submitted to the
XXXth International Conference on High Energy Physics
Osaka, Japan, July 27 - August 2, 2000.

1 Introduction

The measurement of heavy flavour production in two-photon collisions provides a good test of QCD because the large physical scale set by the charm or beauty quark masses makes the perturbative calculations reliable. Many experiments have studied charm production in $\gamma\gamma$ collisions [1-8]. Beauty production in $\gamma\gamma$ collisions has not been measured before since the production of b quarks is expected to be suppressed by more than two orders of magnitude relative to the production of charm quarks. At LEP energies, the direct and resolved processes (Figure 1) give comparable contributions to the cross section [9]. The resolved photon cross section is dominated by the photon-gluon fusion diagram $\gamma \mathrm{g} \to \mathrm{b\bar{b}}$. The production rate of b quarks in two-photon collisions depends on the b quark mass and on the gluon density in the photon.

In this paper we present the preliminary results of the measurements of the $\mathrm{e^+e^-} \to \mathrm{e^+e^-b\bar{b}}$ cross section by the L3 experiment at $\sqrt{s} = 189 - 202$ GeV for a total integrated luminosity of $\mathcal{L} = 410$ pb^{-1}. We identify b quarks by tagging electrons or muons from their semileptonic decays. Two different methods have been utilized for the cross section measurement. In the first approach a cut based analysis is used while in the second the cross section has been estimated from a fit to the transverse momentum of the lepton with respect to the nearest jet.

2 Monte Carlo

For the two photon processes the PYTHIA 5.7 [10] Monte Carlo is used. The non b two photon events are generated with massless ($\mathrm{m_q} = 0$) matrix elements [11] while for b events massive matrix elements are used. The signal events are produced in two separate samples for direct and resolved processes. The resolved process uses the SaS1d photon structure function [12].

The two-photon luminosity function is implemented in the equivalent photon approximation (EPA) with a cutoff: $\mathrm{Q^2} < \mathrm{m}_\rho^2$ [13].

Background sources and their simulated luminosities are $\mathrm{e^+e^-} \to \mathrm{e^+e^-}\tau^+\tau^-$ (1265 pb^{-1}), $\mathrm{e^+e^-} \to \mathrm{Z}/\gamma \to \mathrm{q\bar{q}}$ (15786 pb^{-1}), $\mathrm{e^+e^-} \to \tau^+\tau^-$ (22868 pb^{-1}) and $\mathrm{e^+e^-} \to \mathrm{W^+W^-}$ (59579 pb^{-1}).

These processes are generated with JAMVG [14], PYTHIA 5.7, KORALZ [15] and KORALW [16] respectively.

The detector simulation is performed by a GEANT-based description of the L3 detector [17]. The Monte Carlo events are reconstructed in the same way as the data.

3 Event Selection

3.1 Hadronic Two-Photon Events

The L3 detector has been described in detail in Ref. [18]. The event selection is done in two steps. The first one selects hadronic final states produced in two-photon collisions, the second identifies a b quark by its semi leptonic decay. Hadronic two-photon events are selected by cuts on the number of tracks, the visible energy and the visible mass. The visible energy, $\mathrm{E_{vis}}$, is the sum of the energies measured in the calorimeters and that of the muons measured in the muon spectrometer. The visible mass, $\mathrm{W_{vis}}$, of the event is calculated from the four-momentum vectors of the calorimetric clusters. All particles are considered to be pions except for electromagnetic (EM) clusters identified as photons. We require at least five tracks in each event; the visible energy has to be less than 0.33 $\sqrt{s}$ and the visible mass has to be greater than 3 GeV. The cut on E_{vis} separates the two-photon from annihilation processes which are characterized by high visible energy. The background from $e^+e^- \to e^+e^-\tau^+\tau^-$ and $e^+e^- \to \tau^+\tau^-$ events is suppressed by the five track requirement.

The analysis is limited to untagged events with small photon virtuality. Events are excluded when the most energetic cluster in the small angle calorimeters has an energy greater than 0.4 E_{beam}. Thus the interacting photons are quasi-real: $\langle Q^2 \rangle \cong 0.015$ GeV^2, where $-Q^2$ is the mass squared of the virtual photon.

3.2 Electron Selection

To identify b quarks by their semi leptonic decay to electrons we impose the following cuts similar to the charm selection [19,20]. The analysis is restricted to the polar angle range
$|\cos\theta| < 0.725$

- The distance of closest approach of the track to the average position of the e^+e^- collision point in the plane transverse to the beam must be less than 0.5 mm.
- The electromagnetic cluster is required to correspond to a track; the difference between the azimuthal angle measured from the shower barycentre and from the track impact point at the calorimeter must be smaller than 20 mrad.
- To confirm that the electromagnetic shower is originated by an electron, the distribution of energies measured in the crystals of the calorimeter are compared to that of an EM cluster using a χ^2 test. The cut is $\chi^2 < 3$. In addition two other cuts on shower shape variables are applied. These are $E_1/E_9 > 0.5$ and $E_9/E_{25} > 0.95$ where E_1, E_9 and E_{25} are the energies deposited into the central crystal, 9 and 25 crystals around barycenter respectively.
- The electron candidate must also satisfy the condition $1 - 2\sigma < E_t/p_t < 1 + 2\sigma$, where E_t is the projection of the energy of the cluster on the plane transverse to the beam and p_t is the transverse momentum of the track. The detector resolution σ has different values for data and Monte Carlo; For data σ =0.054 and for Monte Carlo σ =0.046. These values are derived by using data and Monte Carlo samples of $e^+e^- \to e^+e^-e^+e^-$ events.
- To remove photon conversion the invariant mass of the electron candidate and its nearest track should be greater than 0.1 GeV.

Due to the higher mass of b quarks, electrons from the semi leptonic decay of b must have a higher momentum and transverse momentum. This characteristic is used to improve the b purity of the sample by applying the following two cuts:

- The momentum of the electron candidate should be greater than 2.0 GeV. Figure 2 shows the momentum distribution of the electron candidate. In this plot a sample of b events with 5 pb cross section has been added to PYTHIA (udsc) predictions. The theoretical prediction for $b\bar{b}$ cross section is 4.60 pb for a b quark mass of 4.5 GeV. At high momentum, the data are systematicaly higher than the expectations.
- The transverse momentum of the electron candidate with respect to the closest jet axis has to be greater than 1.0 GeV. The jets have been reconstructed using the JADE algorithm with $Y_{cut} = 0.1$. The energy of the electron candidate has been excluded from the jet.

Figure 3 shows the E_t/p_t distribution for the data after applying all the other cuts; The electron peak is very pronounced over a low background.

3.3 Muon Selection

We require the momentum of the muons to be greater than 2.5 GeV and their transverse momentum with respect to the closest jet greater than 1.5 GeV. In order to suppress the contribution from the annihilation processes, we require the muon momentum to be less than 0.2 E_{beam}. The angular acceptance is limited to $|\cos\theta| < 0.9$.

4 The Beauty Cross Section Measurement

The total cross section of inclusive b production is calculated from the following equation:

$$\sigma = \frac{(N^{\mathrm{lept}}_{\mathrm{obs}} - N^{\mathrm{lept}}_{\mathrm{bkg}})\ \pi_{\mathrm{b}}}{\mathcal{L}\ \epsilon_{\mathrm{trig}}\ \epsilon'_{\mathrm{b}}}. \tag{1}$$

The variables are defined as follows:

- $N^{\mathrm{lept}}_{\mathrm{obs}}$ is the number of events in the data after the final lepton selection.
- ϵ_{trig} is the trigger efficiency which is determined from the data using a set of independent triggers.
- $N^{\mathrm{lept}}_{\mathrm{bkg}}$ is the number of background events estimated from Monte Carlo which do not originate from two-photon hadronic interactions.
- $\mathcal{L}$ is the total integrated luminosity.

The b selection efficiency, ϵ'_{b}, is the fraction of b events selected by the lepton tag analysis relative to those generated in the full phase space. The b purity, π_{b}, is defined as:

$$\pi_{\mathrm{b}} = \frac{N^{\mathrm{lept}}_{\mathrm{b}}}{N^{\mathrm{lept}}_{\mathrm{b}} + N^{\mathrm{lept}}_{\mathrm{nb}}}. \tag{2}$$

Where $N^{\mathrm{lept}}_{\mathrm{b}}$ and $N^{\mathrm{lept}}_{\mathrm{nb}}$ represent the number of b and non b events respectively. In order to be independent of the Monte Carlo flavour composition (beauty to non-beauty fraction), the beauty purity can be rewritten as:

$$\pi_{\mathrm{b}} = (1 - \frac{\epsilon_{\mathrm{nb}}}{\epsilon_{\mathrm{d}}})/(1 - \frac{\epsilon_{\mathrm{nb}}}{\epsilon_{\mathrm{b}}}), \tag{3}$$

where the ϵ_{b} (ϵ_{nb}) is the fraction of beauty $N^{\mathrm{lept}}_{\mathrm{b}}$ (non-beauty $N^{\mathrm{lept}}_{\mathrm{nb}}$) events, accepted by the final selection from the b (non b) events obtained after the hadronic selection. The quantity ϵ_{d} is defined by the following relation in which the index (bkg) refers to non two photon backgrounds

$$\epsilon_{\mathrm{d}} = \frac{N^{\mathrm{lept}}_{\mathrm{b}} + N^{\mathrm{lept}}_{\mathrm{nb}}}{N^{\mathrm{had}}_{\mathrm{b}} + N^{\mathrm{had}}_{\mathrm{nb}}} = \frac{N^{\mathrm{lept}}_{\mathrm{obs}} - N^{\mathrm{lept}}_{\mathrm{bkg}}}{N^{\mathrm{had}}_{\mathrm{obs}} - N^{\mathrm{had}}_{\mathrm{bkg}}} \tag{4}$$

.

The equation (4) is obtained by noticing that the total number of selected hadronic events $N_{\mathrm{b}}^{\mathrm{had}} + N_{\mathrm{nb}}^{\mathrm{had}}$ can be expressed as:

$$\frac{N_{\mathrm{b}}^{\mathrm{lept}} + N_{\mathrm{nb}}^{\mathrm{lept}}}{\epsilon_{\mathrm{d}}} = \frac{N_{\mathrm{b}}^{\mathrm{lept}}}{\epsilon_{\mathrm{b}}} + \frac{N_{\mathrm{nb}}^{\mathrm{lept}}}{\epsilon_{\mathrm{nb}}}. \tag{5}$$

This method of deriving the b quark cross section is insensitive to the absolute normalization of the b quark and background Monte Carlo. To estimate ϵ_{nb}, the charm fraction in PYTHIA Monte Carlo is scaled to the measured cross section [21].

5 Beauty Cross Section Results

5.1 Cut Based Analysis

After all cuts are applied 103 electron candidates remain. The trigger efficiency is $94 \pm 3\%$. The background from the annihilation processes and the two-photon production of tau pairs is about 2.5%. We assume that this background has the same trigger efficiency as hadronic two-photon signal events. The beauty purity is 51.0%. The beauty selection efficiency is 1.15%.

The cross section for this channel is:

$$\sigma_{electron-tag}^{ee\rightarrow eebbX} = 11.54 \pm 2.29 \text{ (stat) } \pm 3.40 \text{ (syst) pb}$$

Figure 4 shows the comparison of data and Monte Carlo for the $\mathrm{E_t/p_t}$ distribution when all the cuts for the b selection are applied. In this plot a sample of 11.54 pb of b Monte Carlo events is added to the non b sample of PYTHIA. There is a good agreement between data and Monte Carlo after adding the b events.

As for muons there are 125 candidates in the data. The trigger efficiency is $94 \pm 3\%$ as in the case of electrons. The beauty purity is 50.8%. The beauty selection efficiency is 1.01%. The background from annihilation processes and two-photon production of tau pairs is 5.3%.

The cross section for this decay mode is:

$$\sigma_{muon-tag}^{ee\rightarrow eebbX} = 15.39 \pm 2.86 \text{ (stat) } \pm 4.93 \text{ (syst) pb}$$

The combined cross section for electron and muon channels is:

$$\sigma_{combined}^{ee\rightarrow eebbX} = 13.04 \pm 1.79 \text{ (stat) } \pm 3.59 \text{ (syst) pb}$$

Systematic errors arise from the cut variation, error on charm cross section measurement, trigger efficiency and light quarks background. The dominant systematic error is the cut variation.

5.2 Fit Analysis

An alternative method for measuring b cross section is fitting the data distributions to estimate the b fraction. The transverse momentum of the lepton with respect to the nearest jet, $\mathrm{P_t}$, has been chosen as the fit variable since it has the highest sensitivity to the b fraction. A three parameter fit is applied in which the fractions of b and charm are free parameters. For the fit we assume the following combination of processes:

$$\text{bkgd}+\alpha_{\text{uds}}(\text{uds})+\alpha_{\text{c}}(\text{c})+\alpha_{\text{b}}(\text{b})$$

Where (bkgd), (uds), (c) and (b) are the Monte Carlo distributions of the non two photon backgrounds, events generated with only the light quarks, the c quark and the b quark respectively. α_{uds}, α_{c} and α_{b} are the fractions of (uds), (c) and (b) events respectively; α_{uds} = 1-α_{b}-α_{c}. The fit for electrons is performed on 320 candidates and the b fraction is 29±7%. As for the muons there are 323 candidates for the fit and the b fraction is 55±9%. The higher b fraction for the muon sample is due to the higher cut on momentum. The χ^2/(per degree of freedom) of the electron and muon fits are 12.9/7 and 3.1/7 respectively. The b selection efficiencies are calculated as in the cut based analysis without applying the transverse momentum cut. The b selection efficiency for electrons is 2.20% and for muons is 2.32%. The cross sections are calculated by using these efficiencies and the purities derived from the fit. The fitted distributions are shown in figures 5 and 6.

The resulting cross sections are

$$\sigma^{ee\rightarrow eebbX}_{electron-tag} = 11.10 \pm 2.60 \text{ (stat) } \pm 1.22 \text{ (syst) pb}$$

$$\sigma^{ee\rightarrow eebbX}_{muon-tag} = 18.90 \pm 3.20 \text{ (stat) } \pm 3.40 \text{ (syst) pb}$$

The combined value for the lepton tag is

$$\sigma^{ee\rightarrow eebbX}_{combined} = 14.20 \pm 2.02 \text{ (stat) } \pm 1.56 \text{ (syst) pb}$$

The systematic errors arise from the cut variation, error on charm cross section measurement and trigger efficiency. The P_t of lepton will have different shapes when using massive or massless matrix element Monte Carlos. As a result a new source of systematic has been added due to the different shapes of the two Monte Carlos. This accounts for about 4% of the systematic error for both electrons and muons. The dominant systematic error is the cut variation. Figure 7 shows the measured value of $\sigma_{\text{b}\bar{\text{b}}}$ together with charm cross section measurements.

The experimental results are compared with the theoretical predictions calculated to NLO accuracy. The QCD predictions for this process at $\sqrt{s}$ = 200 GeV are 4.60 pb and 3.89 pb assuming mass of the b quark to be 4.5 GeV and 5.0 GeV respectively.

In conclusion, the $\text{b}\bar{\text{b}}$ cross section measured here for the first time in two-photon collisions, is about 4 standard deviation higher than expected.

Acknowledgments

We wish to express our gratitude to the CERN accelerator divisions for the excellent performance of the LEP machine. We also acknowledge and appreciate the effort of all the engineers, technicians and support staff who have participated in the construction and maintenance of this experiment.

References

[1] JADE Collab., W. Bartel et al., Phys. Lett. B **184**, (1987) 288.

[2] TPC/Two-Gamma Collab., M. Alston-Garnjost et al., Phys. Lett. B **252**, (1990) 499.

[3] TASSO Collab., W. Braunschweig et al., Z. Phys. C **47**, (1990) 499.

[4] TOPAZ Collab., R. Enomoto et al., Phys. Lett. B **328**, (1994) 535, Phys. Rev. D **50**, (1994) 1879, Phys. Lett. B **341**, (1994) 99, Phys. Lett. B **341**, (1994) 238.

[5] VENUS Collab., S. Uehara et al., Z. Phys. C **63**, (1994) 213.

[6] AMY Collab., T. Aso et al., Phys. Lett. B **363**, (1995) 249, Phys. Lett. B **381**, (1996) 372.

[7] ALEPH Collab., D. Buskulic et al., Phys. Lett. B **355**, (1995) 595.

[8] L3 Collab., M. Acciarri *et al.*, Phys. Lett. B **453**, (1999) 83.

[9] M. Drees, M. Krämer, J. Zunft and P.M. Zerwas, Phys. Lett. B **306**, (1993) 371.

[10] T. Sjöstrand, Comput. Phys. Commun. **82**, (1994) 74.

[11] M. Cacciari et al., Nucl. Phys. B **466**, (1996) 173.

[12] G.A. Schuler and T. Sjöstrand, Z. Phys. C **68**, (1995) 607; Phys. Lett. B **376**, (1996) 193.

[13] V. M. Budnev et al., Phys. Rep. **15** (1975) 181.

[14] J.A.M. Vermaseren, Nucl. Phys. B **229**, (1983) 347.

[15] S. Jadach, B.F.L. Ward and Z. Was, Comput. Phys. Commun. **79**, (1994) 503.

[16] M. Skrzypek, S. Jadach, W. Placzek and Z. Was, Comput. Phys. Commun. **94**, (1996) 216.

[17] The L3 detector simulation is based on GEANT Version 3.14; see R. Brun et al., GEANT 3, CERN DD/EE/84-1 (Revised), September 1987 and the GHEISHA program (H. Fesefeld, RWTH Aachen Report PITHA85/02 (1985)) for the simulation of hadronic interactions.

[18] L3 Collab., B. Adeva *et al.*, Nucl. Inst. Meth. **A 289** (1990) 35;
M. Acciarri *et al.*, Nucl. Inst. Meth. **A 351** (1994) 300;
M. Chemarin *et al.*, Nucl. Inst. Meth. **A 349** (1994) 345;
I.C. Brock *et al.*, Nucl. Inst. Meth. **A 381** (1996) 236;
A. Adam *et al.*, Nucl. Inst. Meth. **A 383** (1996) 342.

[19] L3 Collab., A. Andreev, R. McNeil and A. Stone, L3 Note 2263.

[20] A. Stone, Thesis submitted to Louisiana State University (1999).

[21] L3 Collab., A. Andreev and R. McNeil, L3 Note 2548.

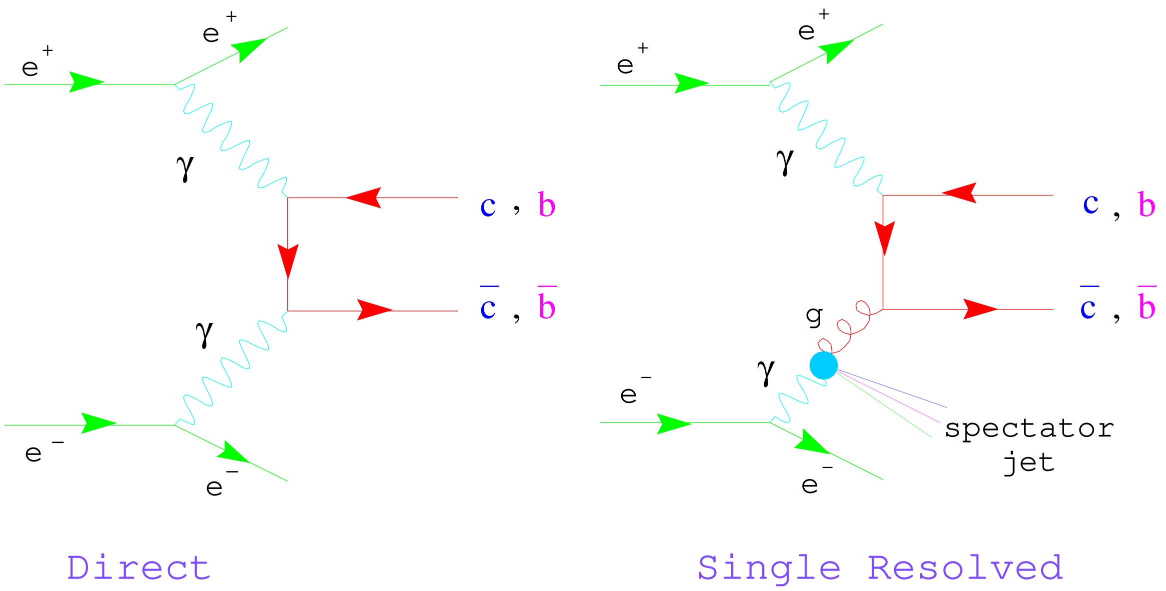

Figure 1: Diagrams contributing to charm production in $\gamma\gamma$ collisions at LEP. Contributions from other processes, double resolved process and VDM, are predicted to be small at LEP energies.

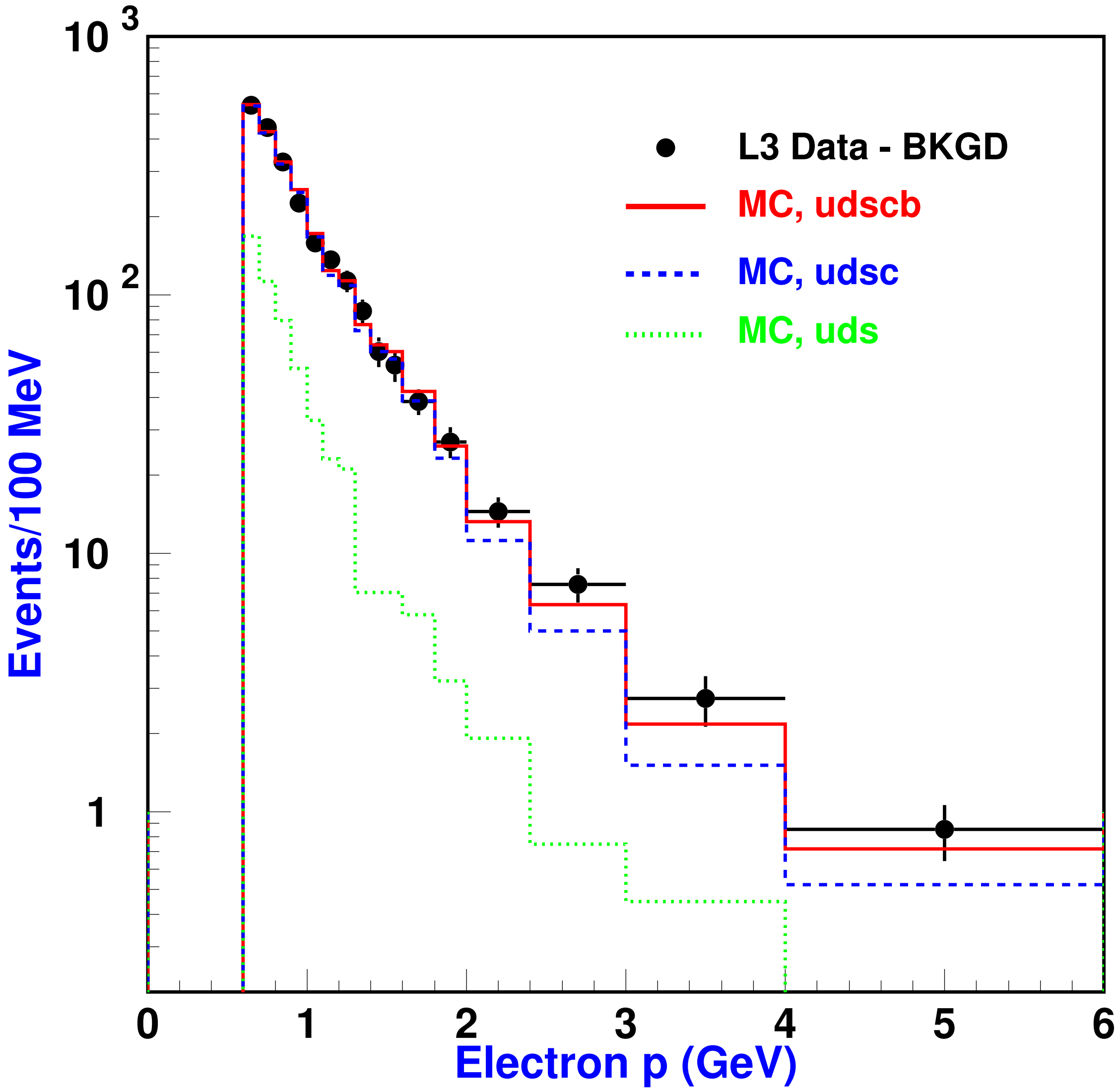

Figure 2: The momentum of the electron candidate. In this plot the dashed histogram is the contribution from PYTHIA Monte Carlo with only u, d, s and c quarks. The c fraction of PYTHIA is scaled to the measured $e^+e^- \to e^+e^-c\bar{c}X$ cross section [21]. In the solid histogram b quark is added to PYTHIA assuming a 5 pb cross section for $b\bar{b}$ (the theory prediction at $\sqrt{s}$ = 200 GeV is 4.60 pb assuming the mass of the b quark to be 4.5 GeV). As can be seen there is sensitivity to the b fraction in the data sample. The plot also indicates that the b cross section must be higher than the expected value of 5 pb.

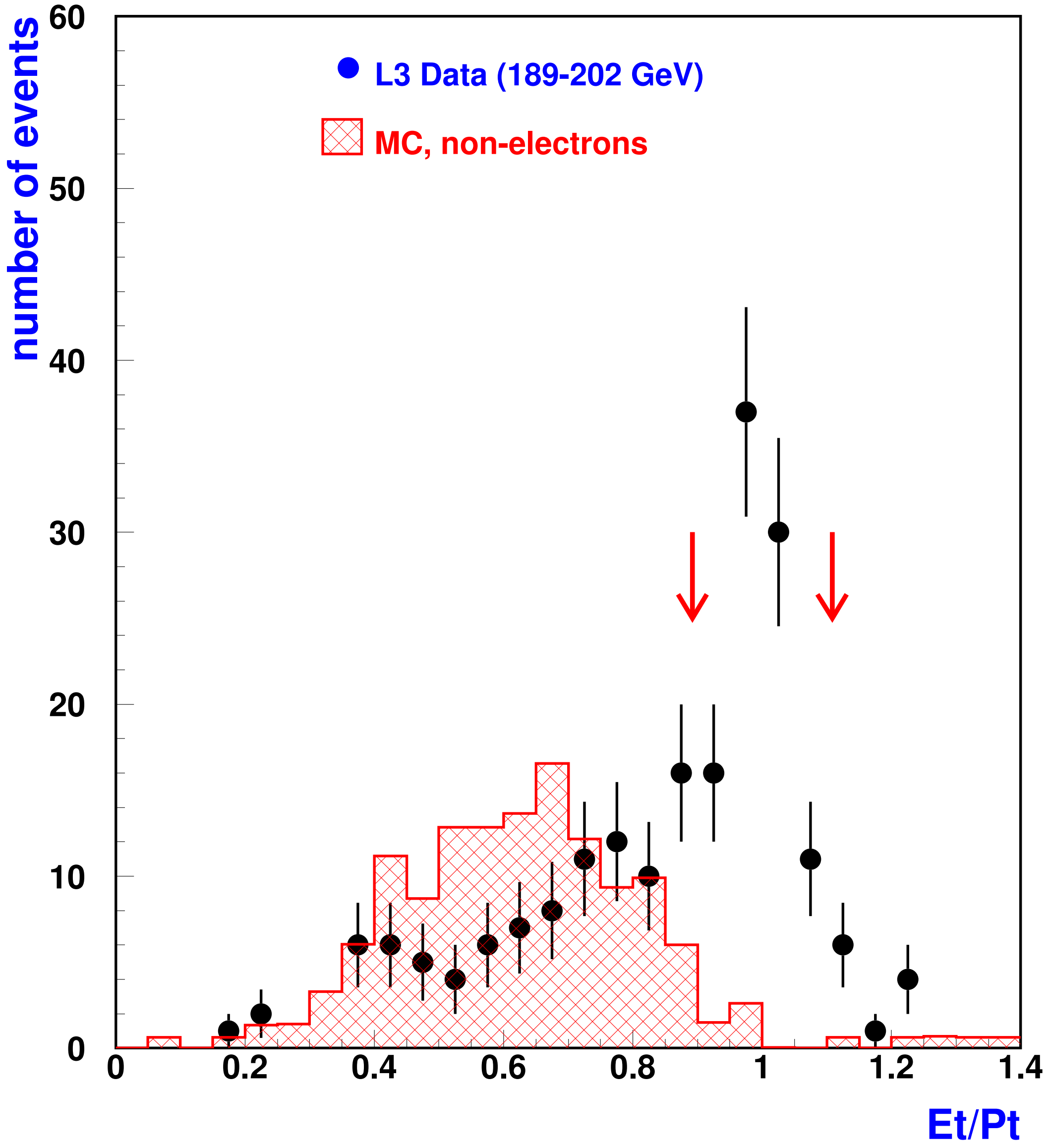

Figure 3: The ratio E_t/P_t for the data electron candidates after applying the b selection cuts. The peak represents the electrons and the arrows show the location of the cuts on this variable. The hatched histogram represents the non electron contribution.

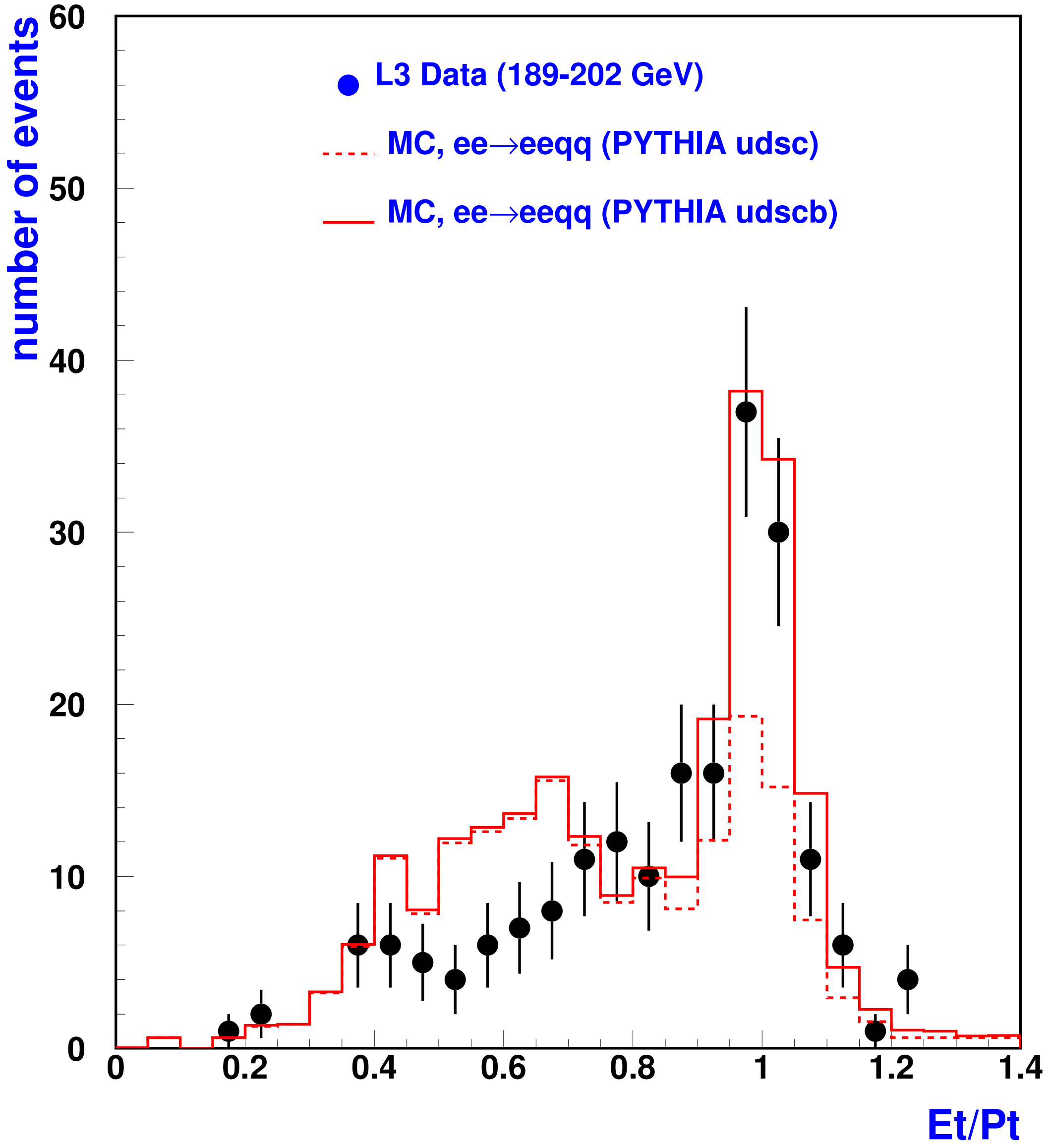

Figure 4: The ratio E_t/P_t for the electron candidates after applying the b selection cuts. The dashed histogram shows the contribution from non b PYTHIA Monte Carlo. The charm fraction of PYTHIA is scaled to the measured cross section. The solid histogram is made by adding the b Monte Carlo to the dashed histogram, according to the measured cross section.

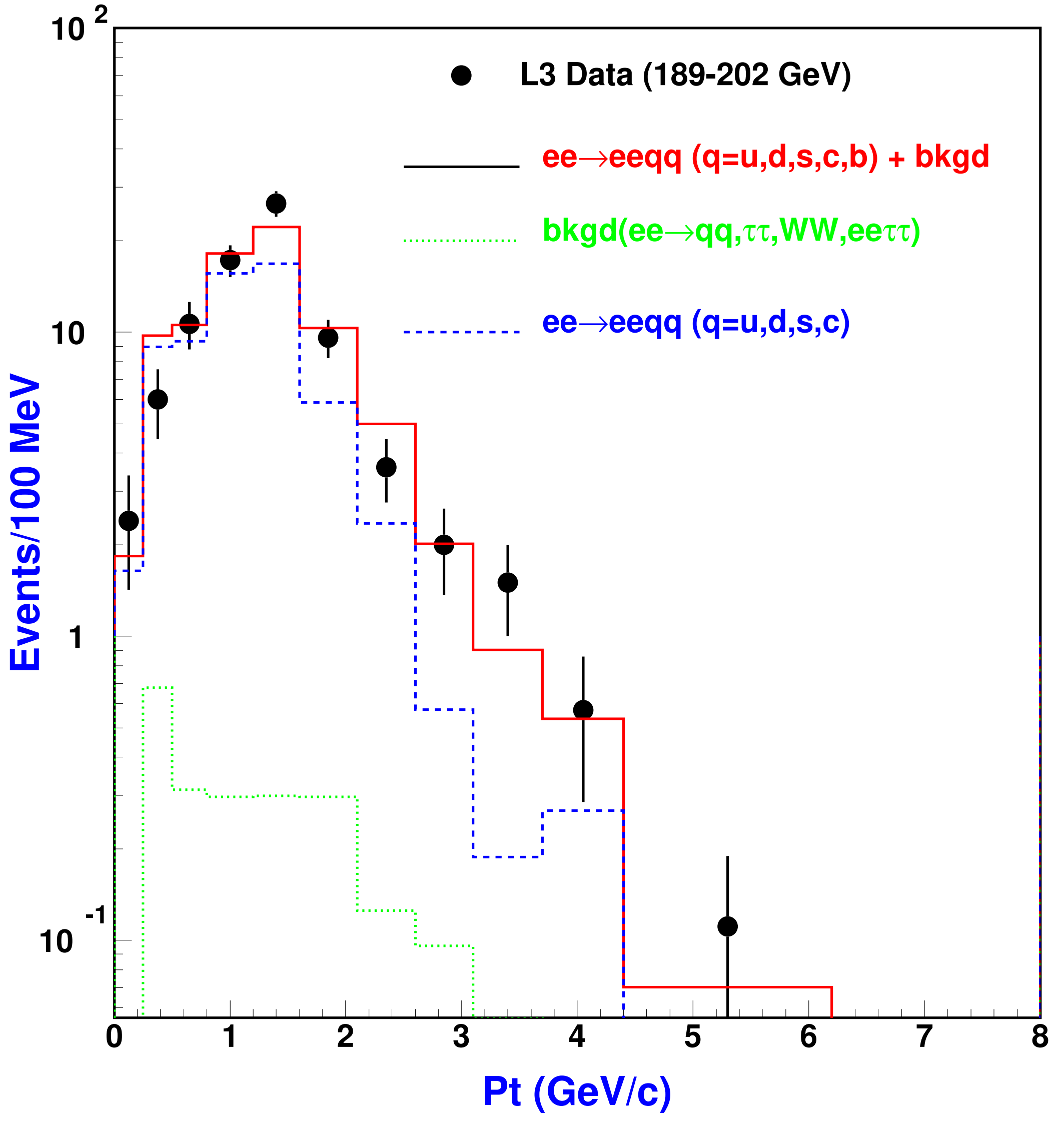

Figure 5: The distribution of the transverse momentum, P_t, of the electron candidate with respect to the closest jet.

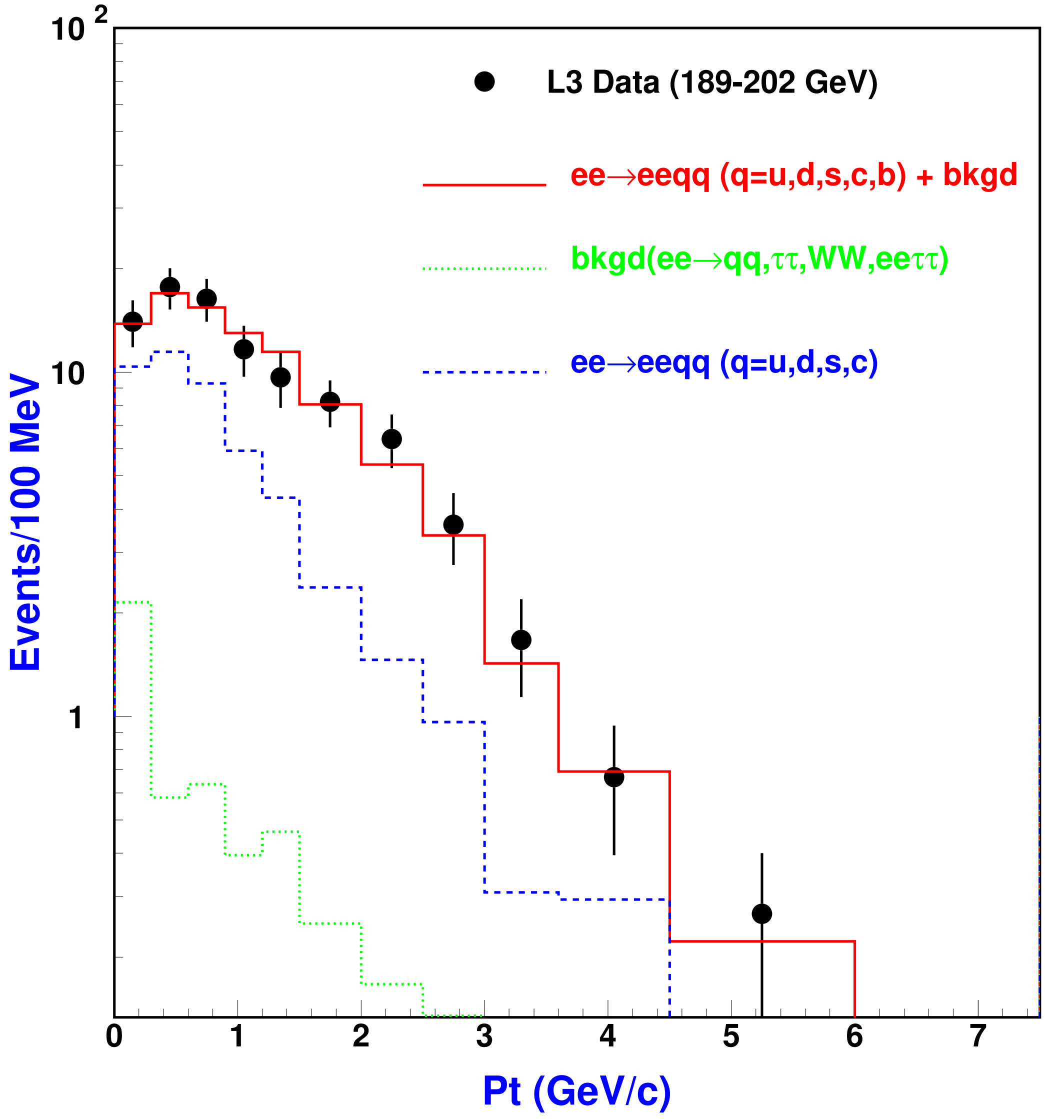

Figure 6: The distribution of the transverse momentum, P_t, of the muon candidate with respect to the closest jet.

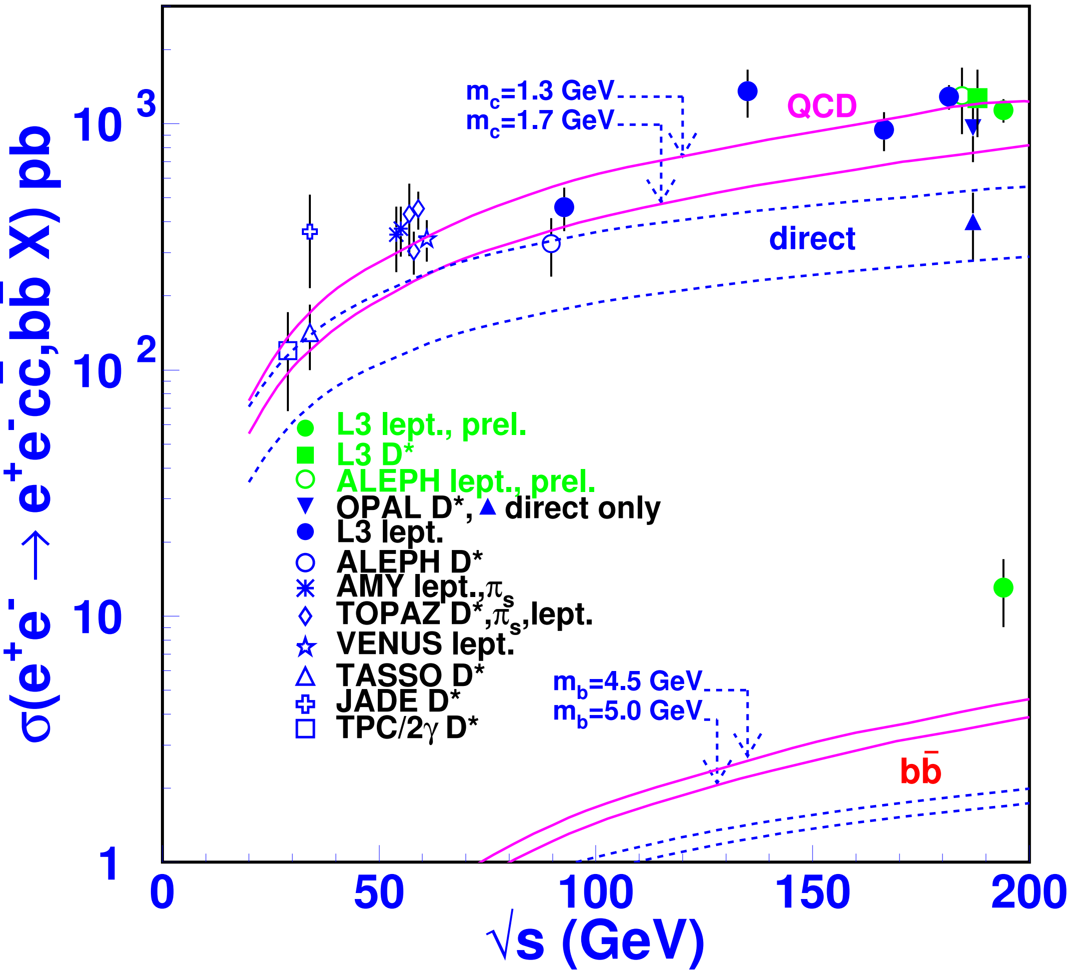

Figure 7: The charm and b production cross section in two-photon collisions. The L3 data from both the electron and the muon events are combined. The statistical and systematic errors are added in quadrature. The dashed line corresponds to the direct process contribution and the solid line represents the QCD prediction for the sum of the direct and resolved processes calculated to NLO. The b cross section is two orders of magnitude smaller than that of charm. The experimental measurement of the b cross section is almost three times higher than the theoretical prediction.